

IMPEDANCE SPECTROSCOPY AND DIELECTRIC RELAXATION IN PHTHALOCYANINE THIN FILM

*Nursel CAN**
*Ahmet ALTINDAL***

Received:11.10.2016; revised:28.03.2017; accepted:16.10.2017

Abstract: Dielectric relaxation behavior of spin coated thin film of novel ball-type binuclear zinc(II) phthalocyanine were studied using impedance spectroscopy technique over a frequency range of 5–13x10⁶ Hz and temperatures (298 – 468 K). Simulation of the obtained impedance data indicated that the dielectric behaviour of the system can be modeled by a parallel RC electrical equivalent circuit. A frequency dependence in the form of ω^m , where the index m is found strongly temperature dependent, was observed for the ac conductivity σ_{ac} . Ac conductivity data were analyzed in terms two different models. The observed temperature dependence of the m indicate that the ac charge transport in Pc film take place via hopping process.

Keywords: Phthalocyanine, Impedance, Relaxation, Ac conductivity, CBH model

Ftalosiyenin İnce Filmde Empedans Spektroskopisi ve Dielektrik Durulma

Öz: Döndürerek kaplama yöntemiyle hazırlanan top tipi çinko (II) ftalosiyenin ince filmlerin dielektrik durulma davranışları 5 Hz. ile 13x10⁶ Hz frekans aralığında sıcaklığa bağlı olarak (298 K – 468 K sıcaklık aralığında) empedans spektroskopisi yöntemiyle incelenmiştir. Elde edilen verilerin modellenmesinde sistemin dielektrik davranışının paralel RC eşdeğer devre ile temsil edilebileceği görülmüştür. Filmlerde ac iletkenliğin frekansa bağlılığının ω^m şeklinde olduğu ve frekansın üssü olan m parametresinin kuvvetle sıcaklığa bağlı olduğu gözlemlenmiştir. Deneysel olarak elde edilen ac iletkenlik verileri iki farklı model kullanılarak analiz edilmiştir. Frekansın üssü olan m parametresinin sıcaklığa bağlılığının incelenmesinde çinko (II) ftalosiyenin ince filmlerde ac yük iletiminin hoplama mekanizması sayesinde gerçekleştiği sonucuna varılmıştır.

Anahtar Kelimeler: Ftalosiyenin, Empedans, Durulma, Ac iletkenlik, CBH model

1. INTRODUCTION

From the point of view of cost, structural flexibility, toxicity, thermal and chemical stability as well as high optical absorption in the visible region ascribe to phthalocyanine (Pc) compounds and their derivatives a unique position among the many other organic materials. Pcs, a wellknown multifunctional organic material for various applications including electronics, optoelectronics, chemical sensor and solar cells (Kimura et al. 1997, Bao et al. 1996, Pandey et al. 2012, Shan Do and Jen Chen, 2007, Altindal et al. 2014). In many applications of phthalocyanines in the thin film form, the determination of the charge transport mechanism and dielectric relaxation process is important to evaluate the usability of these compounds for any specific application. Therefore, understanding of the physical origin of the

*Yıldız Technical University, Faculty of Arts and Sciences, Department of Physics, 34210, İstanbul

**Yıldız Technical University, Faculty of Arts and Sciences, Department of Physics, 34210, İstanbul

Correspondence Author: Nursel Can (can@yildiz.edu.tr)

dielectric behaviour and mechanism of charge transport is essential. A large amount of work can be found in the literature, which have been performed on dc conduction properties of the phthalocyanines with different molecular structures (Manaka and Iwamoto, 2003, Anthopoulos and Shafai, 2003, Khrishnakumar and Menon, 2001, Shafai and Anthopoulos, 2001). On the other hand, there are limited studies on the ac response and dielectric properties of this class of materials. Among the various characterisation techniques, impedance spectroscopy (IS) method is one of the most powerful technique which is widely used to study the structural and dielectric response of the materials as well as for the determination of recombination kinetics in organic based photo-voltaic devices (Piasecki and Nitsch, 2010, Garcia-Belmonte et al. 2010). The main principle of the IS is based on the measurement of the response of the material under test to the sinusoidal stimulus in a wide range of frequency with a small amplitude (Ceyhan et al. 2007). The convertibility of the impedance data to an electrical equivalent circuit make the IS technique a very promising tool MacDonald (1987).

In the present work, in order to investigate its suitability for a particular device application, we focused on the study of conduction mechanism and dielectric relaxation phenomena in thin film of novel ball-type four t-butylcalix Shan Do and Jen Chen, (2007) arene bridged binuclear zinc(II) phthalocyanine (**2**). IS was employed to investigate the charge transport and dielectric relaxation in the film. Strongly frequency and temperature dependent impedance parameters were observed. Nyquist plots show the contribution of grain and grain boundary permittivity in the film.

2. EXPERIMENTAL

The synthesis details of the compound of **2**, shown in Figure 1, were reported elsewhere (Ceyhan et al. 2007). It was synthesized by the tetramerization of 1.3-bis(3.4-dicyanophenoxy)-4-tertbutylcalix[4]arene with $Zn(OAc)_2 \cdot 2H_2O$ in dry DMF at 190 °C.

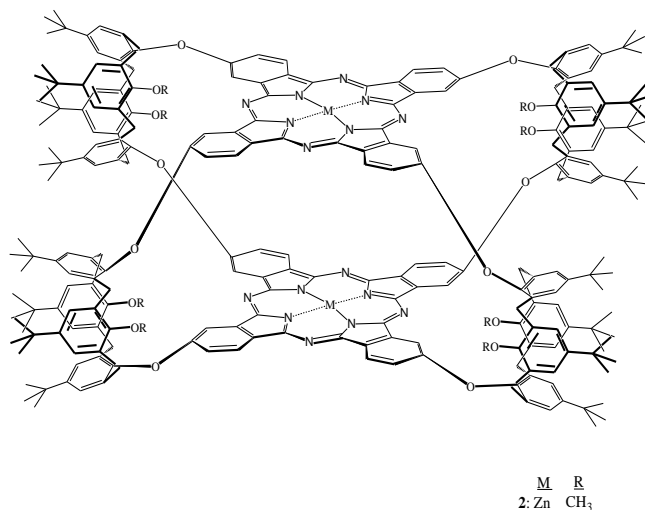


Figure 1:
Structural formula of the compound investigated

For impedance measurements, glass slides with interdigitated gold electrodes (IDEs) were used as substrate. A Schematic diagram of the device structure and photograph of the interdigital electrode array is shown in Fig. 2. The ~ 200 nm thick film of **2** was deposited on IDEs by the spin coating chloroform solution of **2**. For the spin coating processes, 5×10^{-2} M. chloroform solution of the compound was used. The substrate was spun at 1200 rpm for 110 s and then the films were dried at 120 °C for 10 min. Impedance measurements were performed with a HP 4192A impedance analyzer for a frequency range from 5 Hz to 13 MHz. and in the temperature range from 298 K to 468 K. During the impedance measurements a 250 mV

amplitude sine wave was applied to the electrode. A K-type thermocouple was used to determine the temperature of the sample under investigation. Both the impedance and conductivity measurements were carried out under vacuum conditions and in the dark. Experimentally obtained impedance data were collected using a GPIB data transfer card. In order to check the repeatability of the measured data, impedance and conductivity measurements were repeated three times on the same sample and it was observed that the obtained impedance and conductivity data were reproducible with an uncertainty less than 1%.

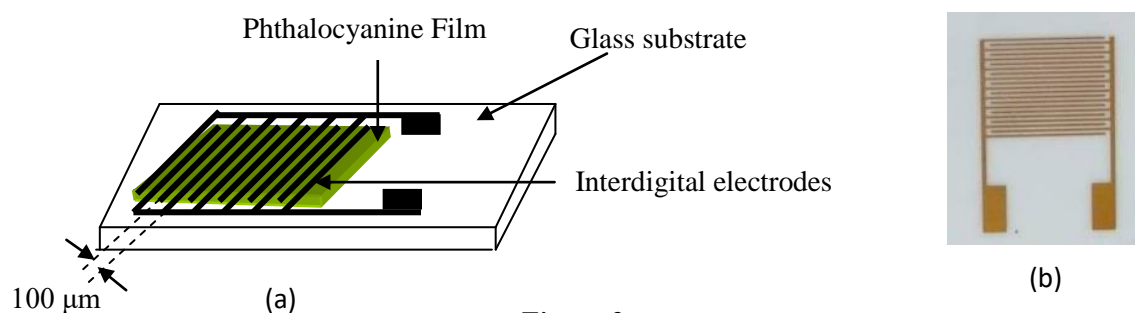


Figure 2:
Schematic diagram of the device (a) and photograph of IDEs (b)

3. RESULTS AND DISCUSSIONS

As known, the measured impedance ($Z^*(\omega)$) of a sample mainly consists of two components; real ($Z'(\omega)$) and imaginary ($Z''(\omega)$) parts and can be expressed as,

$$Z^*(\omega) = Z'(\omega) + jZ''(\omega) \quad (1)$$

In order to estimate the contribution of the bulk and grain boundary effects, the obtained impedance spectra for the film of **2** at different temperatures is depicted in complex plane plot (Figure 3). Figure 3 shows that the pattern of the Nyquist plots are definitely a function of temperature. The appearance of the semicircular shaped curves in impedance spectra mean that the impedance dominated by the capacitive behaviour of the system at low temperatures. It should be mentioned here that the capacitive behaviour of the sample under investigation is not due to the presence of impurities or interfacial phenomena. This behavior can be due to the contribution of the grain and grain boundary to the relaxation time. In the light of the present literature MacDonald (1987), Ceyhan et al. (2006), it can be concluded that the IS of the film of **2** can be modelled with an electrical equivalent circuit as shown in Figure 4(a) at low temperatures. The series resistances R_s represents the losses in the connection cables, R_b and C in the equivalent circuit represent the bulk resistance and capacitance of the film, respectively.

As is clear in Figure 3, with the increase in the sample temperature the response of the film to the sinusoidal stimulus changes significantly and the measured impedance spectra become a series of depressed semicircles with different radius.

The shift in the centre of the arc towards the origin of the Nyquist plot indicates deviation from the Debye dispersion relation and a distribution of relaxation time, rather than a single relaxation time. In the case of non-Debye type of relaxation behaviour, the electrical equivalent circuit of the system under investigation is modified to include a constant phase element (CPE), as shown in Figure 4(b). The inclusion of the constant phase element to electrical equivalent circuit should be interpreted as a slight distribution of relaxation times and inhomogeneity of the Au/Pc interface. In order to identify the contribution of the grain and grain boundary effect, the temperature and frequency dependence of the imaginary impedance was studied in more details (Figure 5). It was found at lower frequencies that, the $Z''(\omega)$ showed monotonic decrease

in the magnitude of $Z''(\omega)$ with increasing frequency at temperatures up to 350 K. The observed $Z''(\omega)$ -f, without any $Z''(\omega)$ peak, reveals that there is no current dissipation in the film in this temperature range. The appearance of a $Z''(\omega)$ maxima at high temperatures confirm the existence of relaxation in the film. It should be noticed here that the frequency at which $Z''(\omega)_{\max}$ occurred, called the relaxation frequency, shifts to higher frequency regions as the temperature increased. This shift in frequency maxima suggesting that the active conduction occur through the grain boundary (Kumar et al. 2009). The decrease in $Z''(\omega)$ maxima and the broadening of the $Z''(\omega)$ peaks with increase in temperature indicates the existence of temperature dependent relaxation phenomena in the film.

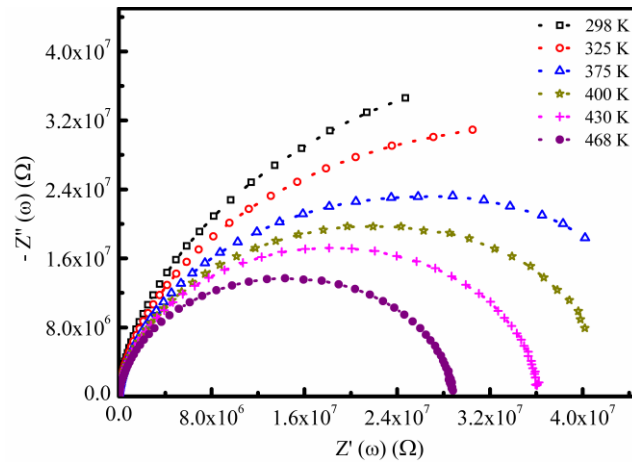


Figure 3:
Nyquist plot ($Z''(\omega)$ vs. $Z'(\omega)$) of the sample at selected temperatures

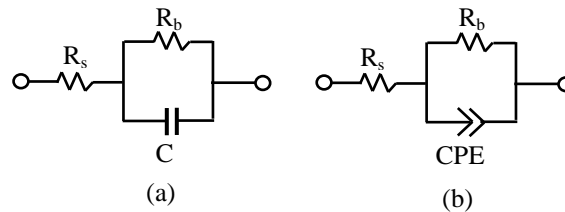


Figure 4:
Electrical equivalent circuits representing (a) low temperature and (b) high temperature IS of the film of 2

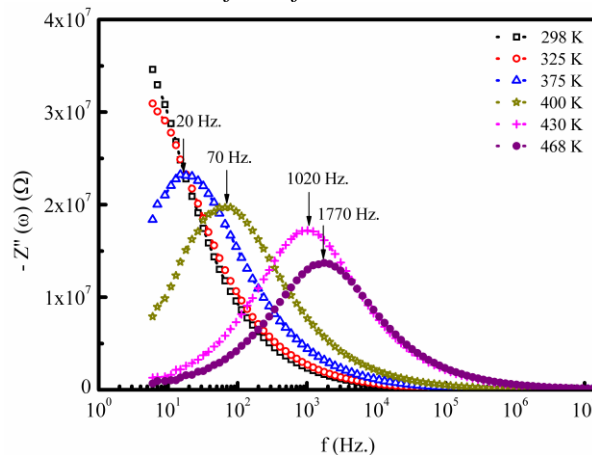


Figure 5:
Variation of the imaginary impedance at indicated temperatures

3.1. Ac Conductivity (σ_{ac}) Study

The variation of the alternating current (ac) conductivity for the compound **2** is shown in Figure 6 at different temperatures. As is clear in Figure 6, at high temperatures, ac conductivity data show a plateau in which ac conductivity frequency independent in low frequency region and exhibits dispersion at higher frequencies. It is also clear from Figure 6 that the temperature dependence of the ac conductivity is stronger at lower frequencies and the value of the frequency at which $\sigma_{ac}(\omega)$ exhibits dispersion shifts to higher frequencies with increase in temperature. If we assume that the mechanism responsible for ac and dc conduction is different and independent from each other, then the measured total conductivity, $\sigma_t(\omega)$, can be expressed as

$$\sigma_t(\omega) = \sigma_o + \sigma_{ac}(\omega) \quad (2)$$

where σ_o is the frequency independent part of the total conductivity (dc conductivity) and the second term represents the frequency dependent part of the conductivity which is related to the dielectric relaxation of the bound charge carriers. Our results indicated that the conduction dominated by the first term in Eq. (2) at low frequencies and high temperature, while the second term becomes more effective at high frequencies and low temperatures. It was found that the overall behavior of the frequency dependent part of the ac conductivity follows the universal power law of the form (Elliot, 1977, Jonscher (1983)).

$$\sigma_{ac}(\omega) = A\omega^m \quad (3)$$

where A is a constant, and the index m is a temperature dependent constant. This type of frequency dependence of the conductivity has also been observed in a broad range of materials including organic semiconductors Altindal (2005) and doped crystalline solid (Leon et al. 1997). In literature, there are a lot of different models which can be used to describe this type of frequency dependence of the conductivity. One of them is the quantum mechanical tunnelling (QMT) model. The basic assumption of the QMT model is that an electron passes through a potential barrier separating the localized sites without acquiring enough energy to pass over the top of the barrier.

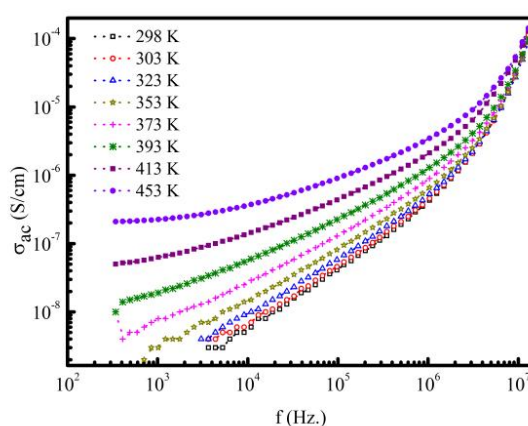


Figure 6:
Frequency dependence of the ac conductivity at indicated temperatures

The QMT model predicts that the frequency and temperature dependence of the measured conductivity should be in the form;

$$\sigma_{ac}(\omega) = \frac{\pi}{3} e^2 kT [D(E_F)]^2 \alpha^{-5} \omega \left[\ln \left(\frac{\nu_0}{\omega} \right) \right]^4 \quad (4)$$

where k is the Boltzmann's constant, T is the temperature, e is the electronic charge, ω is the angular frequency, $D(E_F)$ is localized state density at Fermi level, α is the inverse localization length of wave function for localized states and ν_0 is the characteristic phonon frequency. In this model, the frequency exponent m is given by the following equation;

$$m = 1 - \frac{4}{\ln(\omega\tau_0)} \quad (5)$$

where τ_0 is the characteristic relaxation time of the charge carriers.

The other model, which is developed by Elliot (1977) to explain the ac charge transport in disordered solids, is the correlated barrier hopping (CBH) model. Elliot's hopping model assumes that the charge transport take places via polaron hopping process over the potential barrier separating hopping centres. In this model, the expression for the ac conductivity is

$$\sigma_{ac}(\omega) = \frac{\pi^2 D^2 \varepsilon}{24} \left(\frac{8e^2}{\varepsilon W_0} \right)^6 \frac{\omega^m}{\tau_0^\beta} \quad (6)$$

where W_0 is the optical band gap and ε is the dielectric constant of the material. According to the CBH model the exponent m varies with temperature and frequency. The dependence of m on temperature and frequency is given by (Elliot, 1977)

$$m = 1 - \frac{6kT}{W_0 + kT \ln(\omega\tau_0)} \quad (7)$$

In order to gain insight into the ac conduction mechanism, the values of the exponent m were derived from the slopes of the $\ln(\sigma_{ac}(\omega))$ vs. $\ln(f)$ plot. Figure 7 shows the variation of the values of exponent m with temperature. It is worth mentioning here that the exponent m has values larger than unity. Neither CBH nor QMT models can explain the larger value of m . In order to explain the observed larger exponent, free band conduction model was suggested by (Vidadi et al. 1969)

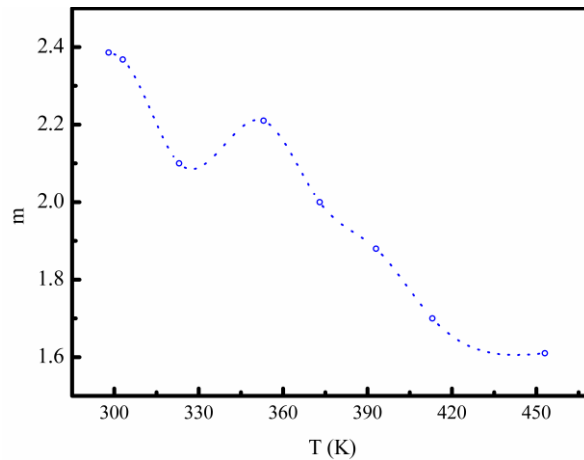


Figure 7:
Variation of the experimentally determine m values with temperature

This model assumes that hopping was believed to occur, and was mainly by free band conductivity with an activation energy of a few tenths of an electron volt. Such type of temperature dependence in m was also observed for other Pc compounds like CoPc (Waclawek et al. 1981). A decreasing trend in m values with increase in temperature is also clear (Figure 7). As mentioned above, if the mechanism responsible for the charge transport in the film of **2** is QMT, the exponent m in this case should be temperature independent. This is not our case, hence QMT model is not appropriate to use as a model to analyse the ac conduction data. Although the temperature dependence of m in agreement with CBH model predictions, the m values larger than unity cannot be explained with CBH model. Larger exponent m reveals that charge transport mechanism is of free band type.

4. CONCLUSION

Impedance spectroscopy technique was employed in order to evaluate the dielectric relaxation mechanism in thin film of **2**. The results show that the impedance spectra strongly temperature dependent especially at the frequencies lower than 10^6 Hz. The observed frequency dependence of $Z''(\omega)$ indicates non-Debye type relaxation in the film. Charge transport properties under ac conditions were also investigated. Analysis of the obtained ac conductivity data indicated that the variation of the frequency exponent m with temperature is in agreement with the prediction of the CBH model. On the other hand, the overall behaviour of m suggests that charge transport mechanism in thin film of **2** is of free band type.

REFERENCES

1. Altındal, A. Abdurrahmanoğlu, Ş. Bulut, M. Bekaroğlu, Ö. (2005) Charge transport mechanism in bis(double-decker lutetium(III) phthalocyanine) (Lu₂Pc₄) thin film. *Synthetic Metals*, 150, 181–187. doi: 10.1016/j.synthmet.2005.02.006
2. Altındal, A. Kurt, Ö. Şengül, A. Bekaroğlu, Ö. (2014) Kinetics of CO₂ adsorption on ball-type dicopper phthalocyanine thin film. *Sensors and Actuators B*, 202, 373–381. doi: 10.1016/j.snb.2014.05.107
3. Anthopoulos, T.D. Shafai, T.S. (2003) Electrical properties of a-nickel phthalocyanine/aluminium interfaces: effects of oxygen doping and thermal annealing. *Journal of Physics and Chemistry of Solids*, 64, 1217–1223. doi: 10.1016/S0022-3697(03)00062-3
4. Bao, Z. Lovinger, A.J. Dodabalapur, A. (1996) Organic field-effect transistors with high mobility based on copper phthalocyanine. *Appl. Phys. Lett.*, 69(20), 3066-3068. doi: 10.1063/1.116841
5. Ceyhan, T. Altındal, A. Erbil, M.K. Bekaroğlu, Ö. (2006) Synthesis, characterization, conduction and gas sensing properties of novel multinuclear metallo phthalocyanines (Zn, Co) with alkylthio substituents. *Polyhedron*, 25, 737–746. doi: 10.1016/j.poly.2005.07.046
6. Ceyhan, T. Altındal, A. Özkaya, A.R. Çelikbıçak, Ö. Salih, B. Kemal Erbil, M. Bekaroğlu, Ö. (2007) Synthesis, characterization and electrochemical properties of novel metal free and zinc(II) phthalocyanines of ball and clamshell types. *Polyhedron*, 26, 4239–4249. doi: 10.1016/j.poly.2007.05.028
7. Eliot, S.R. (1977) A theory of a.c. conduction in chalcogenide glasses. *Philos. Mag.*, 36 (6), 1291-1304. doi: 10.1080/14786437708238517

8. Garcia-Belmonte, G. Boix, P.P. Bisquert, J. Sessolo, M. Bolink, H.J. (2010) Simultaneous determination of carrier lifetime and electron density- of-states in P3HT:PCBM organic solar cells under illumination by impedance spectroscopy. *Solar Energy Materials & Solar Cells*, 94, 366–375. doi: 10.1016/j.solmat.2009.10.015
9. Jonscher, A.K. (1983) *Dielectric Relaxation in Solids*. Chelsea Dielectric Press, London
10. Khrishnakumar, K.P. Menon, C.S. (2001) Determination of the thermal activation energy and grain size of iron phthalocyanine thin films. *Materials Letters*, 48(2001), 64–73. doi: 10.1016/S0167-577X(00)00281-0
11. Kimura, M. Horai, T. Hanabusa, K. Shirai, H. (1997) Electrochromic polymer derived from oxidized tetrakis(2-hydroxyphenoxy)phthalocyaninatocobalt(II) complex. *Chem. Lett.*, 7, 653-654. doi: 10.1246/cl.1997.653
12. Kumar, A. Murari, N.M. Katiyar, R.S. (2009) Investigation of dielectric and electrical behavior in $\text{Pb}(\text{Fe}_{0.66} \text{W}_{0.33})_{0.50}\text{Ti}_{0.50}\text{O}_3$ thin films by impedance spectroscopy. *J. Alloys. Compd.*, 469, 433–440. doi: 10.1016/j.jallcom.2008.01.130
13. Leon, C. Lucia, M.L. Santamaria, J. (1997) Correlated ion hopping in single-crystal yttria-stabilized zirconia. *Phys. Rev. B.*, 55, 882-887. doi: 10.1103/PhysRevB.55.882
14. MacDonald, J.R. (1987) *Impedance Spectroscopy: Emphasizing Solid Materials and Systems*, Wiley-Interscience, New York
15. Manaka, T. Iwamoto, M. (2003) Electrical properties of unsubstituted/fluorine-substituted phthalocyanine interface investigated by Kelvin probe method. *Thin Solid Films*, 438–439, 157–161. doi: 10.1016/S0040-6090(03)00726-0
16. Pandey, R. Zou, Y. Holmes, R.J. (2012) Efficient, bulk heterojunction organic photovoltaic cells based on boron subphthalocyanine chloride-C70. *Applied Physics Letters*, 101, 033308-1-033308-4. doi: 10.1063/1.4737902
17. Piasecki, T. Nitsch, K. (2010) Study of sprayed coatings and compound materials by impedance spectroscopy. *Surface & Coatings Technology*, 205, 1009-1014. doi: 10.1016/j.surfcoat.2010.07.074
18. Shafai, T.S. Anthopoulos, T.D. (2001) Junction properties of nickel phthalocyanine thin film devices utilising indium injecting electrodes. *Thin Solid Films*, 398–399, 361–367. doi: 10.1016/S0040-6090(01)01345-1
19. Shan Do, J. Jen Chen, P. (2007) Amperometric sensor array for NO_x, CO, O₂ and SO₂ detection. *Sensors and Actuators B.*, 122, 165–173. doi: 10.1016/j.snb.2006.05.030
20. Vidadi, Y.A. Rozenshtein, L.D. Chistyakov, E.A. (1969) Hopping and band conductivities in organic semiconductors. *Sov. Phys. Solid State*, 11, 173-175.
21. Waclawek, W. Kulesza, M. Zabkowska, M. (1981) *Mater. Sci. (Poland)*, 7, No:2-3, 385.